BIOINFORMATICS

Vol. 00 no. 00 2006
Pages 1–10

A Decompositional Approach to Parameter Estimation in Pathway Modeling: A Case Study of the Akt and MAPK Pathways and Their Crosstalk

Geoffrey Koh [a], Huey Fern Carol Teong [b], Marie-Véronique Clément [b], David Hsu [c], P.S. Thiagarajan [c]

[a]Graduate School for Integrative Sciences and Engineering, National University of Singapore
[b]Department of Biochemistry, National University of Singapore
[c]Department of Computer Science, National University of Singapore

ABSTRACT

Parameter estimation is a critical problem in modeling biological pathways. It is difficult because of the large number of parameters to be estimated and the limited experimental data available. In this paper, we propose a decompositional approach to parameter estimation. It exploits the *structure* of a large pathway model to break it into smaller components, whose parameters can then be estimated independently. This leads to significant improvements in computational efficiency. We present our approach in the context of Hybrid Functional Petri Net modeling and evolutionary search for parameter value estimation. However, the approach can be easily extended to other modeling frameworks and is independent of the search method used. We have tested our approach on a detailed model of the Akt and MAPK pathways with two known and one hypothesized crosstalk mechanisms. The entire model contains 84 unknown parameters. Our simulation results exhibit good correlation with experimental data, and they yield positive evidence in support of the hypothesized crosstalk between the two pathways.

Contact: thiagu@comp.nus.edu.sg

1 INTRODUCTION

Computational models and methods are becoming an integral part of molecular biology. They are being used not only to identify cellular components, but also to determine how these components interact with one another. Quantitative modeling of these interactions will play an important role in understanding fundamental intra- and inter-cellular processes. In particular, quantitative modeling of the dynamics of biological pathways has drawn much attention recently (Chen *et al*., 2003; Matsuno *et al*., 2003; Ye *et al*., 2005). Our focus here is on modeling the dynamics of intra-cellular signaling pathways.

Thanks to rapid technological advances, the structures of many signaling pathways are now available. Using this information, attempts to derive system models that capture the *dynamics* of these pathways are beginning to emerge. For such attempts to be successful, several challenges must be addressed.

First, choosing a modeling framework is important, because it determines the appropriate level of abstraction at which cellular components and their interactions can be described. The choice of the modeling framework is also strongly influenced by the simulation and analysis tools that the framework offers.

Independent of the framework chosen, modeling the dynamics of a signaling pathway requires the determination of various reaction rate constants that control the bio-chemical reactions constituting the pathway. These rate constants are usually called model parameters. Almost always, only a few of these parameters can be determined directly through experiments. The rest must be estimated, based on experimental data, e.g., gene expression or protein concentration measurements. Unfortunately, the amount of data available is rather limited in quantity and sometimes corrupted by noise. This, combined with the large number of unknown model parameters makes the parameter estimation problem computationally difficult and sometimes intractable.

In this work, we adopt the recently introduced Hybrid Functional Petri Net (HFPN) (Matsuno *et al*., 2003) as the modeling framework and propose a *decompositional* approach to the parameter estimation problem in signaling pathway modeling. The biological application driving our study is the Akt and MAPK pathways *and* their hypothesized crosstalk mechanisms.

A key advantage of our decompositional approach is that it exploits the structure of a large pathway model to break it into smaller components, whose parameter estimation problem can then be solved independently. This leads to significant improvements in computational efficiency due to the reduction in the dimensionality of the search space and in the number of local minima. For the Akt-MAPK pathways with 84 unknown parameters, our approach produced reasonable estimates for all parameters in about 18 hours. In comparison, the common approach, which estimates all the parameters together, cannot even finish after running for 4 days.

We present our decompositional approach in the context of the HFPN modeling framework and evolutionary search (Beyer *et al*., 2002) for parameter value estimation. However, it can be easily extended to other modeling frameworks, such as simultaneous systems of differential equations, hybrid automata, etc. (Sorribas *et al*., 1988; Ye *et al*., 2005). Our approach is also independent of the specific search method used for parameter estimation. In fact, one may choose different search methods for different components, if this improves computational efficiency.

We have chosen HFPN as the modeling framework, because it captures both continuous and discrete behaviors that are inherent in biological systems. Another advantage for our purposes is that the

underlying graph of an HFPN model naturally captures the information flow and the dependency relations among the basic elements of a pathway. This allows us to systematically decompose a pathway model into components.

We tested our method on the Akt-MAPK pathways, based on data from 27 experiments. This pathway model has a total of 84 unknown parameters. Our method succeeded in decomposing it into 6 components, each of which has no more than 25 unknown parameters, which must then be estimated together. Our estimated parameters produced fairly good simulation results when compared with experimental data. We also used our model with its estimated parameters to check the plausibility of the hypothesized crosstalk between the protein PDK1 of the Akt pathway and the protein MEK of the MAPK pathway.

The rest of this paper is organized as follows. In Section 2, we review background information on the HFPN modeling framework and the Akt-MAPK pathways. We also provide some pointers to related work on parameter estimation techniques. In Section 3, we describe the HFPN model of the Akt-MAPK pathways and encapsulate the crosstalk hypothesis in the model. In Section 4, we present the details of our decomposition method for parameter estimation. In Section 5, we present simulation results to validate the estimated parameter values and to test the crosstalk hypothesis. In Section 6, we discuss some issues and possible improvements of our current decomposition method. Finally, in Section 7, we summarize the main results and discuss the prospects for future work.

2 THE BACKGROUND

There are many approaches to modeling biological pathways (de Jong, 2002). We first explain the modeling framework that we have chosen and then the specific signaling pathway setting in which we have carried out our parameter estimation work.

2.1 Hybrid Functional Petri Nets

Petri nets are a fundamental model of distributed discrete event systems (Reisig, 1992). They offer an appealing visual notation which resembles the graphical notations often deployed by biologists to depict the components and their interactions in biological pathways. The Petri net model, however, has a precise semantics which fixes the meanings of the nodes and the arcs of the model as well as its *dynamics*.

A Petri net can be viewed as a bipartite graph with two kinds of nodes, usually called *places* and *transitions*. The places represent local states and the transitions represent local change-of-states. Entities called tokens are used to mark the places to specify the current distributed state of the system. The transitions, according to a *firing rule* associated with them, effect local transformations of the token distribution to model the system evolving from the current state to a new one. In the graphical representation, the places are drawn as circles, the transitions as boxes, and the tokens as small bullets placed inside the places. A standard firing rule is that if all the places pointing into the transition currently carry at least one token each, then the transition may fire. When it does so, one token is removed from each of its input places and one token is added to each of its output places. To improve modeling power, one can also associate *weights* with the arcs so that the firing of a transition can depend on, remove and add multiple tokens from its surrounding places. This is illustrated in Figure 1(b). There are a large number of variations

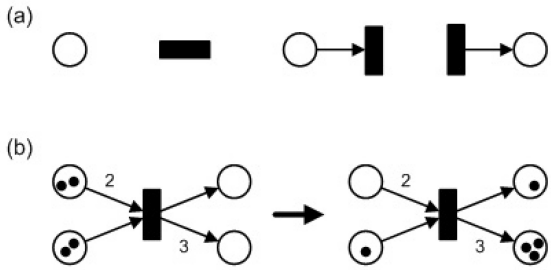

Fig. 1. (a)The basic components and connections of a Petri net model. (b) Change in markings of a Petri net due to the firing rules.

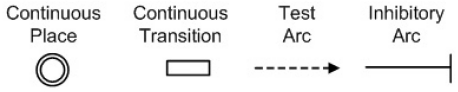

Fig. 2. Additional features of an HFPN model.

of this basic model, and they have been deployed in a wide variety of application domains. A recent collection of such efforts in biological settings can be found in Chen *et al*. (2003); Matsuno *et al*. (2003); Voss *et al*. (2003); Zevedei-Oancea *et al*. (2003).

The classical Petri net is a model of a discrete event system whereas a crucial aspect of biological pathways is the various biochemical reactions which are best specified as continuous differential equations. Indeed, both discrete and continuous features appear to be an integral part of fundamental biological processes (Lincoln *et al*., 2004). To account for this, various *hybrid* dynamic models have been proposed in the literature (Lincoln *et al*., 2004). In the setting of Petri nets, the hybrid version of interest to us is the Hybrid Functional Petri Net developed by Matsuno *et al*. (2003).

In an HFPN, places and transitions can be discrete or continuous. The marking associated with a continuous place can be a real number, which can change smoothly according to the speed assigned to the continuous transition(s) to which it serves as an input or output place. In addition, an edge can be one of three types: normal, inhibitory, or test. An inhibitory edge points from a discrete place to a transition, and it specifies that the transition is inhibited from firing whenever a token is *present* in the place. A test edge from a place to a transition specifies that the transition can only fire if a token is present in the place, *but* the firing of the transition does not change the token count on this place. See Figure 2 for HFPN features that are not present in ordinary Petri nets.

A typical biochemical equation depicting an enzyme catalyzed reaction can be written as Equation 1. In this reaction, the enzyme E binds reversibly to the substrate S, before converting it into the product P and releasing it. The parameters k_1, k_2 and k_3 are the rate constants that govern the speed of these reactions.

$$S + E \underset{k_2}{\overset{k_1}{\rightleftharpoons}} S.E \xrightarrow{k_3} E + P \tag{1}$$

The HFPN representation of such a reaction is shown in Figure 3(a). Each molecular type is represented by a continuous place, and its concentration corresponds to the marking associated

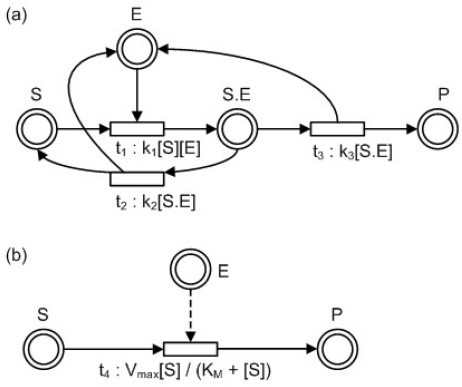

Fig. 3. (a) HFPN representation of the biochemical reaction. Assuming Michaelis-Menton kinetics, the model can be simplified into (b).

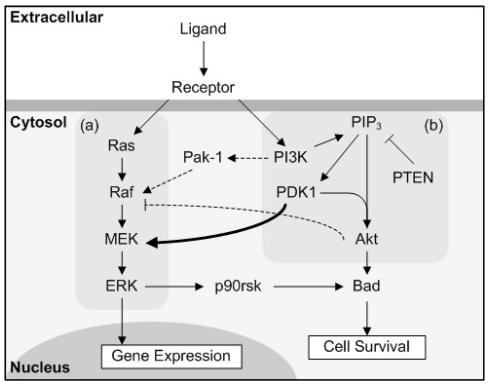

Fig. 4. Schematic of the (a)MAPK pathway, (b)Akt pathway and their crosstalk interactions. Known crosstalk interactions are marked with dashed arrows while the hypothesized interaction is marked with a bold arrow.

with that place. The continuous transitions then represent the reactions. Each continuous transition is associated with a function which determines the speed of firing. In a biological setting, the rate of a reaction is often a function of its reactants' concentration level (denoted as [E], [S], and [E.S], respectively). In an HFPN model, this function will be attached to the continuous transition.

Assuming quasi-steady-state approximations, the HFPN model can be simplified into Figure 3(b). The function of the transition will be expressed as the Michaelis-Menton equation $V_{max}[S]/(K_M + [S])$ where

$$V_{max} = k_3[E] \quad \text{and} \quad K_M = \frac{k_2 + k_3}{k_1}$$

We have adopted the HFPN to model the Akt and the MAPK pathways and their crosstalk. Our choice of this formalism has been influenced by the fact that it serves as the front-end of the software Cell Illustrator with which the HFPN-based models can be simulated (Nagasaki *et al*., 2003). In many settings, an attractive alternative is the *hybrid automata* modeling framework (Henzinger, 1996) with its direct use of differential equations to capture the continuous dynamics. This model has an extensive theory and an emerging set of simulation, analysis, and verification tools (Lincoln *et al*., 2004). It has been used to study, for instance, the excitable behavior of cardiac cells (Ye *et al*., 2005), Delta-Notch protein signaling (Ghosh *et al*., 2001) and quorum sensing in bacteria (Alur *et al*., 2001).

2.2 The Akt Pathway

The kinase Akt plays an important role in the regulation of cellular functions. Its downstream targets include kinases, transcription factors and other regulatory molecules (Khwaja, 1999). Akt has also been identified as a major factor in many types of cancer. The schematic describing the Akt pathway, its interactions with the mitogen-activated protein kinase (MAPK) pathway, and their downstream targets are shown in Figure 4.

The activation of the Akt signaling pathway is a multi-step process (Bellacosa *et al*., 1998). When ligands such as fibroblast growth factors, epidermal growth factors and insulin bind to their specific membrane receptors, the cytosolic domains of the receptors will undergo conformational changes, allowing them to act as scaffolds for certain types of proteins in the cell. Phosphoinositide 3-kinase (PI3K) is one such protein that gets recruited and as a result, its catalytic subunit will be activated. The activated PI3K will then phosphorylate the membrane phospholipid phosphatidylinositol-4,5-biphosphate (PIP_2) at the 3-OH position to phosphatidylinositol-3,4,5-triphosphate (PIP_3) and this is tightly regulated by the phosphatase and tensin homolog (PTEN), which removes the phosphate group from the same position.

PIP_3 recruits Akt and the phosphoinositide-dependent kinase-1 (PDK1) to the plasma membrane allowing the phosphorylation of Akt by PDK1. Akt is activated by a sequential phosphorylation at its threonine residue 308 (Thr^{308}) and serine residue 473 (Ser^{473}) by PDK1 and an unknown kinase (named PDK2) respectively (Nicholson *et al*., 2002). Activated Akt further phosphorylates and activates its downstream targets such as Forkhead transcription factor (FKHR) and glycogen synthase kinase 3β (GSK-3β).

Another important molecular target for Akt signaling is Bad, a protein that regulates apoptosis. Bad can bind to the anti-apoptotic proteins Bcl-2 and Bcl-XL, allowing the pro-apoptotic protein Bax to oligomerize at the mitochondria and promote the release of cytochrome c into the cytosol. This would lead to the activation of caspases and cell death. Upon phosphorylation by Akt at the Ser^{136} residue, Bad is sequestered in the cytosol by 14-3-3 proteins, thus Bcl-2 and Bcl-XL can bind to Bax, hence preventing the release of cytochrome c and inhibiting apoptosis. Constitutive Akt signaling promotes cell survival and proliferation, leading to the formation of tumors.

2.2.1 MAPK Crosstalk The significance of the Akt pathway lies not only in the several cellular functions it regulates, but also in its interactions with other pathways (Heldin, 2001). The MAPK signaling cascade is one such pathway that is influenced by components of the Akt pathway.

The MAPK pathway is a highly conserved pathway that is linked to mitogenic responses and cell proliferation. It can be activated by a wide range of growth factors and hormones and it too has several target molecules. Some of the signals that activate the Akt pathway can also activate the MAPK pathway. Upon activation, the tyrosine residues of the receptor is phosphorylated, serving as docking sites for proteins such as Grb2 and SOS. The exchange factor SOS then replaces guanosine 5'-diphosphate (GDP) on the Ras protein with guanosine 5'-triphosphate (GTP), thus activating it. Activated Ras

then binds to the protein Raf, triggering a wave of downstream phosphorylation where Raf activates the MAPK kinase (MEK) which in turn activates p44/42 MAPK (ERK).

Recent studies show that the Akt pathway can regulate the MAPK pathway by competitively phosphorylating Raf at Ser^{259} (Moelling *et al*., 2002), preventing further activation. However, this Akt-MAPK regulation is not entirely inhibitory. PI3K has been shown to activate Raf via the intermediate protein PAK-1 (Chaudhary *et al*., 2000). Recently, Sato *et al*. (2004) have shown that PDK1 is involved in the activation of MEK. Moreover, our data also shows that the repression of PDK1 gene expression using small interference RNA (siRNA) leads to a decrease in activated MEK and ERK in a prostate cancer model (Teong *et al*., 2006). Thus these support our hypothesis that PDK1 could be involved in the activation of MEK by phosphorylating it, as indicated by a bold arrow in Figure 4.

2.3 Parameter Estimation

Various techniques based on global optimization have been proposed for estimating the parameters of pathway models (see, e.g., Kikuchi *et al*., 2003; Moles *et al*., 2003). However, these techniques, which usually estimate all the model parameters together, do not scale up well for large pathway models with many parameters, due to the high dimensionality of the search space and the presence of many local minima.

For larger pathway models, it is natural to try to decompose it into small, independent components and estimate the parameters for each component separately, thus reducing the computational complexity. The general idea of model decomposition for parameter estimation has been successfully applied in many domains, e.g., Bayesian model learning (Neapolitan, 2003), geometric curve fitting (Jiang *et al*., 2005), control of large dynamical systems (Williams *et al*., 1998), etc.

In related work on Akt and MAPK pathways (Hatakeyama *et al*., 2003), a simplified model based on simultaneous differential equations is proposed. The model has about 30 unknown rate parameters, which are estimated with an in-house genetic algorithm. There is no report of computation time required. It is also not clear how much experimental data was used and how the estimated parameters were validated. To ease the computational burden, in subsequent work (Kimura *et al*., 2004), the model is decomposed *manually* based on the observation that parameters in upstream components of enzyme catalyzed reactions can be estimated independent of parameters in downstream components, if there are no feedback loops connecting them. Our decompositional approach uses a similar observation, but is more general, as it is not restricted to enzyme catalyzed reactions. It is also fully automatic.

3 THE HFPN MODEL OF THE AKT-MAPK PATHWAYS

We have modeled the Akt pathway and the MAPK pathway as well as the hypothesized crosstalk as an HFPN model. The full structure of the model is shown in Figure 5. The parameters associated with the transitions and the initial protein concentration levels are shown in Table 1 and Table 2. In Table 1, the four parameters whose values have been taken from literature are marked with a * while the remaining parameters have values that have been estimated by our technique. The sources of information of the four known parameters can be found in: http://www.comp.nus.edu.sg/∼rpsysbio/ismb2006.

Table 1. Rate reactions and their associated parameters. The Michaelis-Menton constants (K_M) are given in nM. The maximal rate constants (V) are expressed in nM.s^{-1}. The first order and second order rate constants (k) are given in s^{-1} and nM^{-1}.s^{-1} respectively.

No	Rate Equation	Parameter	
1	$k_1[R]$	$k_1 = 0.01$	
2	$k_2[R_{act}]$	$k_2 = 0.002$	
3	$k_3[R_{int}]$	$k_3 = 0.001$	
4	$k_4[R_{act}][PI3K]/(Km_4 + [PI3K])$	$k_4 = 0.3$	$Km_4 = 78$
5	$V_5[PI3Ka]/(Km_5 + [PI3Ka])$	$V_5 = 46.2$	$Km_5 = 117$
6	$k_6[PI3Ka][PIP_2]/(Km_6 + [PIP_2])$	$k_6 = 0.05$	$Km_6 = 6170$
7	$k_7[PTEN][PIP_3]/(Km_7 + [PIP_3])$	$k_7 = 5.5$	$Km_7 = 80.9$
8	$k_8[PIP_3][AKT_{cyto}]$	$k_8 = 0.045$	
9	$k_9[PIP_3.AKT]$	$k_9 = 0.089$	
10	$k_{10}[PDK1][PIP_3.AKT]/(Km_{10} + [PIP_3.AKT])$	$k_{10} = 20$	$Km_{10} = 80000^*$
11	$k_{11}[PP2A][PIP_3.AKTp]/(Km_{11} + [PIP_3.AKTp])$	$k_{11} = 0.037$	$Km_{11} = 8800$
12	$k_{12}[PDK2][PIP_3.AKTp]/(Km_{12} + [PIP_3.AKTp])$	$k_{12} = 20$	$Km_{12} = 80000^*$
13	$k_{13}[PP2A][PIP_3.AKTpp]/(Km_{13} + [PIP_3.AKTpp])$	$k_{13} = 0.04$	$Km_{13} = 48000$
14	$k_{14}[PP2A][PIP_3.AKTpp]/(Km_{14} + [PIP_3.AKTpp])$	$k_{14} = 0.163$	$Km_{14} = 48000$
15	$k_{15}[R_{act}][Ras]/(Km_{15} + [Ras])$	$k_{15} = 50$	$Km_{15} = 20000$
16	$V_{16}[Rasa]/(Km_{16} + [Rasa])$	$V_{16} = 15000$	$Km_{16} = 7260$
17	$k_{17}[Rasa][Raf]/(Km_{17} + [Raf])$	$k_{17} = 0.09$	$Km_{17} = 50$
18	$k_{18}[Pakp][Raf]/(Km_{18} + [Raf])$	$k_{18} = 0.183$	$Km_{18} = 500$
19	$V_{19}[Rafp]/(Km_{19} + [Rafp])$	$V_{19} = 78$	$Km_{19} = 30$
20	$k_{20}[PIP_3.AKTpp][Rafp]/(Km_{20} + [Rafp])$	$k_{20} = 0.1$	$Km_{20} = 13.2$
21	$k_{21}[Rafp][MEK]/(Km_{21} + [MEK])$	$k_{21} = 5.6$	$Km_{21} = 7200$
22	$k_{22}[PDK1_{cyto}][MEK]/(Km_{22} + [MEK])$	$k_{22} = 0.04$	$Km_{22} = 2600$
23	$k_{23}[PP2A][MEKp]/(Km_{23} + [MEKp])$	$k_{23} = 0.45$	$Km_{23} = 1250$
24	$k_{24}[Rafp][MEKp]/(Km_{24} + [MEKp])$	$k_{24} = 5.17$	$Km_{24} = 24500$
25	$k_{25}[PDK1_{cyto}][MEKp]/(Km_{25} + [MEKp])$	$k_{25} = 0.05$	$Km_{25} = 2150$
26	$k_{26}[PP2A][MEKpp]/(Km_{26} + [MEKpp])$	$k_{26} = 0.4$	$Km_{26} = 4316$
27	$k_{27}[MEKpp][ERK]/(Km_{27} + [ERK])$	$k_{27} = 0.089$	$Km_{27} = 52000$
28	$k_{28}[MKP3][ERKp]/(Km_{28} + [ERKp])$	$k_{28} = 30$	$Km_{28} = 160$
29	$k_{29}[MEKpp][ERKp]/(Km_{29} + [ERKp])$	$k_{29} = 0.0308$	$Km_{29} = 55000$
30	$k_{30}[MKP3][ERKpp]/(Km_{30} + [ERKpp])$	$k_{30} = 32$	$Km_{30} = 60$
31	$k_{31}[ERKpp][P90RSK]/(Km_{31} + [P90RSK])$	$k_{31} = 0.0017$	$Km_{31} = 97.6$
32	$k_{32}[ROS][P90RSK]/(Km_{32} + [P90RSK])$	$k_{32} = 0.76$	$Km_{32} = 181$
33	$V_{33}[P90RSKp]/(Km_{33} + [P90RSKp])$	$V_{33} = 468$	$Km_{33} = 2.8$
34	$k_{34}[P90RSKp][Bad]/(Km_{34} + [Bad])$	$k_{34} = 0.798$	$Km_{34} = 10$
35	$k_{35}[Pakp][Bad]/(Km_{35} + [Bad])$	$k_{35} = 0.04$	$Km_{35} = 30000$
36	$V_{36}[Badp112]/(Km_{36} + [Badp112])$	$V_{36} = 821$	$Km_{36} = 43300$
37	$k_{37}[PIP_3.AKTpp][Bad]/(Km_{37} + [Bad])$	$k_{37} = 0.397$	$Km_{37} = 20700$
38	$k_{38}[Pakp][Bad]/(Km_{38} + [Bad])$	$k_{38} = 0.04$	$Km_{38} = 30000$
39	$V_{39}[Badp136]/(Km_{39} + [Badp136])$	$V_{39} = 821$	$Km_{39} = 43300$
40	$k_{40}[PI3Kp][Bax]/(Km_{40} + [Bax])$	$k_{40} = 0.0659$	$Km_{40} = 42000$
41	$k_{41}[Bax_{cyto}]$	$k_{41} = 0.0148$	
42	$k_{42}[Bad][Bcl2]$	$k_{42} = 0.0561$	
43	$k_{43}[Bcl2.Bad]$	$k_{43} = 0.0624$	
44	$k_{44}[Bax][Bcl2]$	$k_{44} = 0.002^*$	
45	$k_{45}[Bcl2.Bax]$	$k_{45} = 0.02^*$	
46	$k_{46}[NOX5]$	$k_{46} = 0.00038$	
47	$k_{47}[ROS]$	$k_{47} = 0.0155$	
48	$k_{48}[ROS][PI3Kp][Pak]/(Km_{48} + [Pak])$	$k_{48} = 0.14$	$Km_{48} = 482$
49	$V_{49}[Pakp]/(Km_{49} + [Pakp])$	$V_{49} = 83000$	$Km_{49} = 29100$
50	$k_{50}[PIP_3][PDK1_{cyto}]$	$k_{50} = 0.0007$	
51	$k_{51}[PDK1]$	$k_{51} = 0.98$	

Table 2. Initial concentration of the cellular components.

Place	Concentration (nM)
R	80
PI3K	100
PIP_2	7000
PTEN	0.1
AKT_{cyto}	200
$PDK1_{cyto}$	1000
PDK2	3
PP2A	150
RAS	18900
RAF	66.4

Place	Concentration (nM)
MEK	36500
ERK	34900
MKP3	2.4
P90RSK	5
BCL2	100
BAD	100
BAX	100
NOX5	2000
ROS	200
PAK	500

The model can be viewed as separate modules interacting with one another via shared nodes. Figure 5(a) models the reactions that take place when the receptors are activated by external signals (indicated by the place 'Serum'). It also includes the reactions of the Akt pathway. A point to note is that under prolonged activation, the cells become desensitized to the signals and respond less to it. We have modeled this phenomena as receptor internalization (Reaction 2).

The MAPK pathway is depicted by Figures 5(b),(c) and (d). After activation by the receptors, Ras will catalyze the phosphorylation of

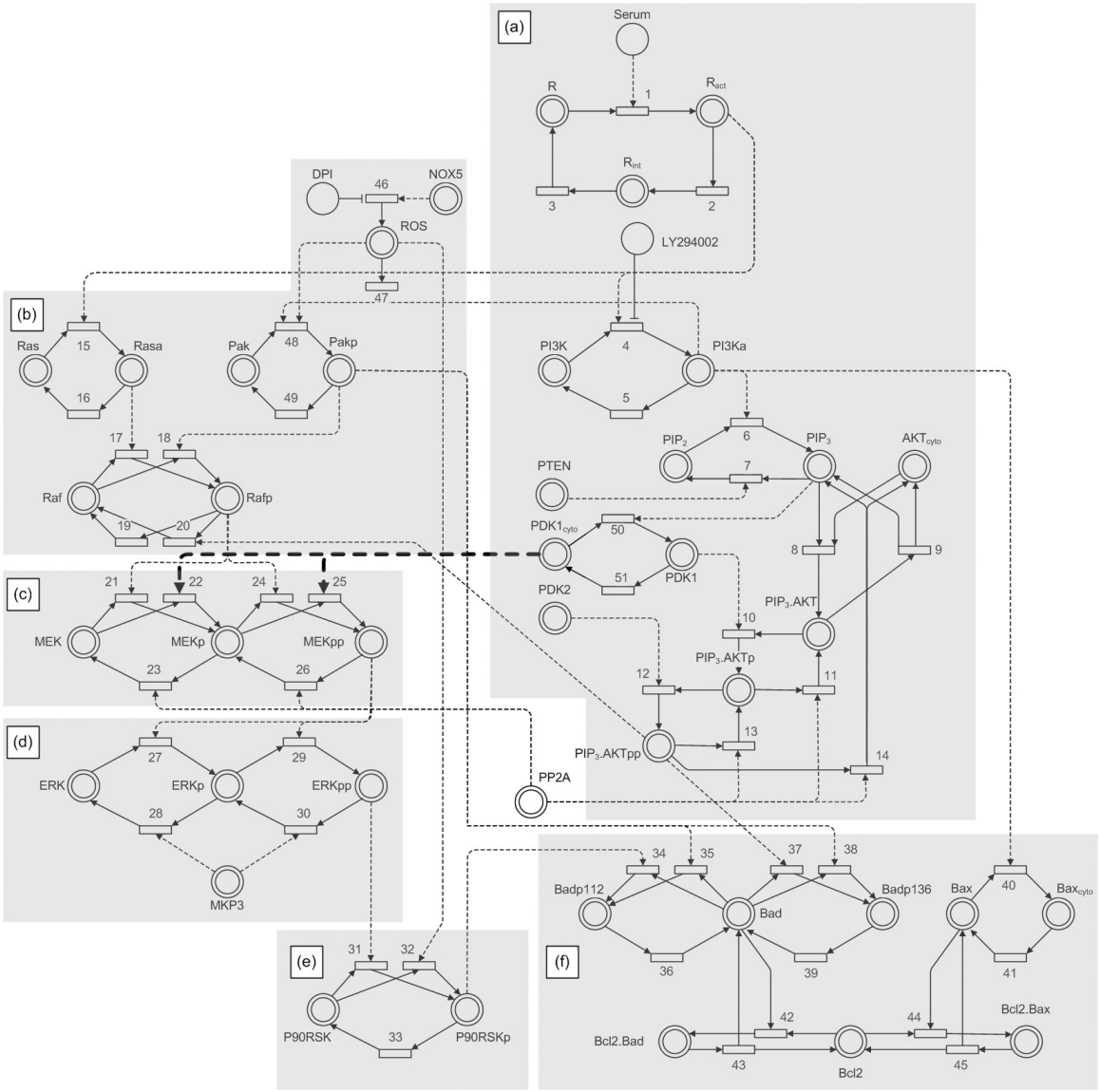

Fig. 5. HFPN model of the Akt and MAPK pathways. The hypothesized crosstalk interaction is emphasized by bold test arcs. The members of downstream components should include the places of the upstream components which they are directly linked from. However to reduce clutter, we show the components as separate modules.

Raf. Phosphorylated Raf, denoted as 'Rafp', will then phosphorylate MEK at two sites, forming the doubly phosphorylated MEKpp (Figure 5(c)). Finally, ERK will be phosphorylated by MEKpp in the same manner, as shown in Figure 5(d).

In our model, there are three possible paths for crosstalk interactions: Active PI3K can upregulate the phosphorylation of Raf via PAK1(Reactions 48 and 18). Akt can inhibit Raf activity (Reaction 20), and PDK1 can affect MEK phosphorylation (Reactions 22 and 25) by the hypothesized interactions. The protein PP2A is an ubiquitous phosphatase which reverses the action of several kinases in our pathway. Hence it is not considered as exclusively belonging to the Akt pathway or the MAPK pathway.

Figure 5(f) models the activity of the Bcl-2 family members, which include the proteins Bcl-2, Bad and Bax. As mentioned in the previous section, these proteins play important roles in regulating apoptosis. It has also been shown that ERK can regulate Bad phosphorylation through the activation of the protein P90RSK, shown in Figure 5(e).

Our model consists of 44 places connected to 51 transitions. For most of the transitions, their dynamics are driven by Michaelis-Menton equations (e.g. Reactions 4, 5, 6). The rest are either association/dissociation reactions (e.g. Reactions 42, 43) or synthesis/degradation reactions (e.g. Reactions 46, 47) whose rates are governed by the mass action laws. Each of these reactions have one or two parameters associated with them.

4 PARAMETER ESTIMATION

Parameter estimation can be viewed as an optimization problem with differential-algebraic constraints. The input to the problem consists of the values of state variables at selected discrete time points. In the present setting, these are steady-state or time-series measurements of protein concentration levels. The problem is to determine the values of the m parameters $\mathbf{p} \in \mathbb{R}_+^m$ and all the unknown protein concentration levels such that they minimize the following objective function:

$$J(\mathbf{p}) = \sum_{i,j,t_e} \sqrt{\frac{(x_{ij}(t_e, \mathbf{p}) - x_{ij}^{\text{exp}}(t_e))^2}{w_{ij}^2}} \tag{2}$$

subject to

$$\dot{\mathbf{x}} = f(\mathbf{x}, t) \tag{3}$$

$$h(\mathbf{x}, t) \geq 0 \tag{4}$$

$$\mathbf{p}^L \leq \mathbf{p} \leq \mathbf{p}^U \tag{5}$$

Here f is the set of differential constraints describing the system dynamics. h is the state constraints for the variables $x \in \mathbf{x}$ for all $t \in [0, T]$. $\mathbf{p}^L$ and $\mathbf{p}^U$ are the lower and upper bound constraints on the parameters $\mathbf{p}$. The time points $t_e \in T_e \subset [0, T]$ describe the set of time instances where experimental data are available. The expression $x_{ij}(t_e, \mathbf{p})$ is the model predicted value of the variable x_i in experiment j at time t_e using parameters $\mathbf{p}$ while $x_{ij}^{\text{exp}}(t_e)$ is the experimental measurement of the same variable. w_{ij} is the weight that is used to normalize the contributions of each term to the objective function. This value is usually taken to be the maximum value of x_i in experiment j.

A typical parameter estimation algorithm starts by randomly choosing parameter values from the search space $\mathbb{R}_+^m$. It uses (3) to simulate the system according to the chosen parameters and then uses (2) to compare the results with the input data. The results of this comparison provide the information to improve the parameter values through gradient descent or stochastic search (Pardalos *et al*., 2002). This process repeats until a better solution can no longer be found or a pre-specified maximum number of iterations is reached.

Our optimization problem is highly non-linear and we will use the evolution strategies algorithm to solve this problem. This algorithm keeps a working set of μ candidate solutions. Each solution consists of a vector of parameter values. In each iteration, it randomly selects two parent solutions from the working set and generates a new one, possibly by interpolating the values of parent vectors. Thereafter, it alters the values slightly and scores the new solution by simulating the model according to these parameter values and applying the objective function. A number of such solutions are generated and from the combined set, the best scoring μ solutions are selected for the next iteration. This carries on for a certain number of iterations, or until no better solutions can be obtained (Beyer *et al*., 2002).

Common approaches to parameter estimation try to estimate all the parameters together. This leads to a high-dimensional search space and hence to very high computational complexity. The key feature of our approach is to exploit the *structure* of a pathway, to break down the parameter estimation problem into a series of smaller problems. The structure of a pathway model determines the causal links and dependencies between the system variables. We use this dependency relationship to extract pathway components that can be handled independently.

This decompositional approach can be applied to different modeling frameworks. Furthermore, it is independent of the specific search method (Beyer *et al*., 2002; Kirkpatrick *et al*., 1983; Moles *et al*., 2003) used for parameter optimization. Here we present our method in the context of the HFPN model combined with evolutionary search (Beyer *et al*., 2002).

4.1 Pathway Decomposition

The goal of pathway decomposition is to extract components from the pathway model whose parameter estimation problems can be solved independently. A component is an executable subgraph of the HFPN model. By an "executable" subgraph we mean a subgraph that can be simulated as a model by itself, assuming we have the values for the parameters and initial conditions relative to the nodes in this subgraph. It is not difficult to see that a component is executable if and only if its set of nodes (places and transitions) are *closed* relative to the full model in the following sense. If a place node is present in the component, all its incoming transitions must also be present in the component. Furthermore, all the transitions to which the place is connected via normal arcs must also be present in the component. This is so since the reactions associated with these transitions are precisely those that determine the concentration levels of the protein associated with the place. If a place is connected to a transition via an inhibitory arc or a test arc then the reaction associated with the transition does not affect the concentration level of the place in any way. By similar reasoning, if a transition is present in a component, all its input places must also be in the component.

Since there are many components (the whole model itself is a component), we must choose them in a systematic fashion so as to help decompose the parameter estimation problem. To do so, we first color the nodes of the model. We then compute a component using the criterion to be described below. We then solve the parameter estimation problem for this component. This is followed by updating the colors of some of the nodes. We then proceed to compute a second component and so on.

As a first step, we assign colors to each place. We assume we have experimental data that has been produced by K experiments conducted under different conditions. With each place we associate a K-dimensional color vector. Suppose the jth experiment produces time series values and/or the steady state concentration level of the protein associated with the place p. Then the jth component of the color vector of p is set to be grey. Otherwise it is fixed to be white. If one or more components of the color vector of a place is grey then the color of the place is defined to be grey. Otherwise it is defined to be white.

The transitions are initially colored as follows. Due to the nature of the reactions being represented by the transitions, each transition can have one or two rate parameters associated with it. If all the parameters associated with a transition are known, then the transition is colored black. If none of the parameters associated with a transition are known then it is colored white. If one but not both the parameters associated with a transition are known, then it is colored grey.

To see how we choose our first component, let $H = (P, T, h, C, a)$ be an HFPN where

- P is the set of places,
- T is the set of transitions,

- $h : P \cup T \rightarrow \{\text{discrete}, \text{continuous}\}$ labels the places and the transitions as being discrete or continuous.
- $C \subseteq \{(P \times T) \cup (T \times P)\}$ is the set of arcs.
- $a : C \rightarrow \{\text{normal}, \text{test}, \text{inhibitory}\}$ labels arcs as being normal, test or inhibitory.

Let p be a grey colored place. Then a particular component containing p -let us denote this component as $comp(p)$- is defined to be the least set of nodes of H satisfying the following conditions.

(C1) $p \in comp(p)$.

(C2) Suppose $x \in comp(p) \cap P$ and x is colored grey or white and (y, x) is an arc in H then y is also in $comp(p)$.

(C3) Suppose $x \in comp(p) \cap T$ and (y, x) is an arc in H then y is also in $comp(p)$.

(C4) Suppose $x \in comp(p) \cap P$, x is colored grey or white, (x, y) is an arc in H and (x, y) is a normal arc, then y is also in $comp(p)$

It is easy to see that $comp(p)$ is indeed a component. Now from among all components $\{comp(p)\}$ where p ranges over the set of grey places, we choose the one which has a minimum number of white/grey transitions while maximizing the number of grey places. Thus choosing a component is a non-trivial task. A number of strategies can be adapted to ease this task but we will not address them here. In any case, this part of the procedure consumes only a small fraction of the overall time needed.

Suppose we have chosen the component $comp(p_0)$ corresponding to the grey place as the best according to our criterion. In the model shown in Figure 5, p_0 is PIP_3.AKTpp and the component it generates is highlighted in Figure 5(a). We now apply the evolutionary search procedure to $comp(p_0)$ using a reserved fraction of the experimental data that provides values for the concentration levels of the proteins associated with the grey places in $comp(p_0)$. This search involves simulating the component several times, adjusting the parameters in each iteration to get a better result according to the specifics of the evolutionary procedure which we will not get into detail here. During this phase, the estimation procedure might get stuck in a local minima while significantly differing from the reported data. Such situations are dealt with in two possible ways. The first consists of using biological intuition to bump the current estimated parameter values out of the local minima trap. The second is to examine the concerned experimental data and discard it as being too noisy or as being improperly conditioned to be reliable.

At the end of this first phase, all the parameters associated with the transitions in $comp(p_0)$ would have been estimated. We now color all the nodes in $comp(p_0)$ as black.

We now choose a suitable grey place p_1 in $P - comp(p_0)$ and compute $comp(p_1)$ and repeat the above process. It is worth noting that when computing $comp(p_1)$, black-colored places of $comp(p_0)$ will form the boundary nodes of this new component. This is because, according to our back-tracing procedure for computing components, the input transitions of a black-colored place will *not* be included in the new component. This implies that each new component will include only a small portion of components that have already been computed. This leads to reduced computation time for each of our parameter estimation task.

After a finite number of iterations all the parameters would have been estimated and all the nodes would have been colored black. For the model shown in Figure 5, the sequence of components chosen is (a), (b), (c), (d), (e) and (f).

We then check the accuracy of the estimated parameters by simulating the model using the estimated parameters and the fraction of the experimental data that has been reserved for this purpose.

5 SIMULATION AND RESULTS

We now describe our results on parameter estimation (Section 5.1) and on the hypothesized Akt-MAPK crosstalk mechanisms (Section 5.2).

5.1 Parameter Estimation

Using the method described in the previous section, we performed parameter estimation for the Akt-MAPK pathways. The data for the estimation problem was obtained from 27 experiments, of which 10 provided time-series data and 17 provided steady-state data. The 27 experiments were performed under 18 different initial conditions. We used data from 23 experiments as inputs to our parameter estimation procedure and reserved data from 4 time-series experiments to validate the results of estimation. The data reserved for validation was not revealed to the estimation procedure. All the data files that we used are available for download from http://www.comp.nus.edu.sg/∼rpsysbio/ismb2006.

The Akt-MAPK pathways consist of 51 reactions and a total of 88 parameters, of which 4 are known. We assume that the initial conditions for all the places are known, and this is supported partly by experimental data. For other situations where not all the initial values are known, the missing protein concentrations can be treated as parameters to be estimated as well.

We ran the estimation procedure on a Pentium 4 PC with a 2.8GHz processor and 2.5GB memory. Our procedure broke the pathways into 6 components (Figure 5(a)-(f)). The average time to estimate the parameters for each component was about 3 hours, and the total time to estimate all the parameters was about 18 hours.

For comparison, we also tried to solve the same parameter estimation problem using the global approach; in other words in which one tries to estimate all the parameters together using the evolutionary search method. On the same computational platform, after running for 4 days, the global method failed to produce a set of parameters that can produce reasonable simulation results. See Figure 6 for a comparison.

An obvious measure to assess the accuracy of the parameters and the reliability of the parameter estimation method is the deviation

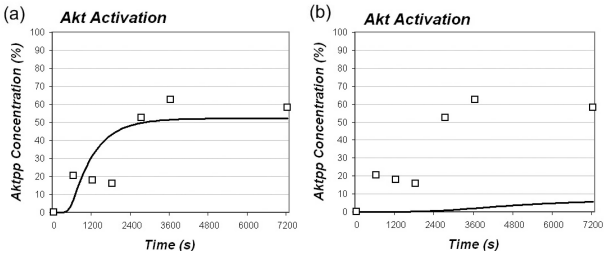

Fig. 6. Comparison of the simulation results of Akt against experimental data using the parameters estimated with (a) the decompositional method and (b) the conventional method. ('□' - experimental data points, '—' simulation profiles).

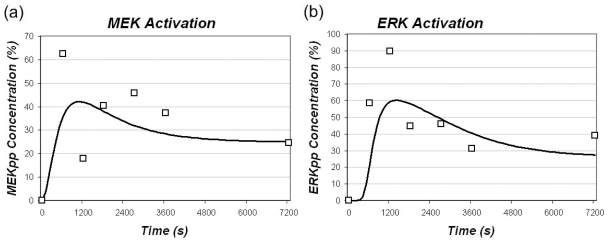

Fig. 7. Simulation profiles of (a) MEK and (b) ERK activation levels.

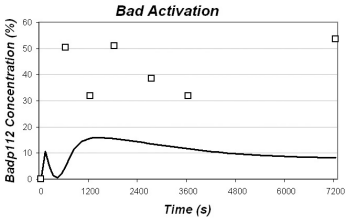

Fig. 8. Simulation profiles of Bad activation levels compared to experimental data.

of the simulation results from experimental data. Figure 7 shows the simulation results of both MEK and ERK activity and Figure 8 shows the Bad phosphorylation levels for the experiment where the cells are treated with diphenyleneiodonium (DPI), a NADPH oxidase inhibitor, in the presence of serum. Due to the lack of space, we do not show the results for all the proteins here. Figure 7 shows that the match between the simulation results and experimental data is good, though not perfect. Given the limited, noisy data available and the high dimensionality of the search space, these results represent a reasonable first step. We expect that as we generate better data both in terms of quantity and quality, a better match will be obtained. Longer running time for the estimation procedure may also potentially help.

Among the results obtained, we indeed have cases in which the match between the simulation results and experimental data is not good. Figure 8 shows the simulation results and experimental data for phosphorylated Bad. There is a systematic, constant difference between them. From a static analysis of the model in Figure 5, the inhibition of the production of superoxide (ROS) by treatment with DPI will propagate downstream and we would expect the level of phosphorylated Bad at Ser^{112} to decrease (Figure 5(f)). However, the experimental data points for activated Bad in Figure 8 are consistently higher than those from the cells which have not been treated with DPI. This difference could be due to unknown reactions and needs to be further investigated.

5.2 Effects of PDK1 on MEK and ERK

A key biological motivation for this work was to test the plausibility of the hypothesized crosstalk interaction between the Akt and the MAPK pathways. Experiments show that in LNCaP, a prostate cancer cell line (Horoszewicz *et al*., 1983), transfected with PDK1 siRNA, which reduces the total PDK1 in the cell, results in a significant decrease in the phosphorylation of MEK and ERK. This suggests a possible crosstalk with PDK1 activating MEK by phosphorylation. We performed the same simulations, decreasing the

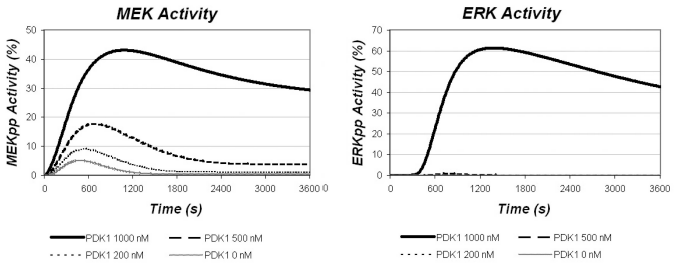

Fig. 9. Simulation of MEK and ERK activation levels with decreasing amounts of PDK1.

levels of PDK1 (from 1000 nM to 0 nM) to mimic the knock-down of PDK1 using siRNA. Figure 9 shows the results of the simulations. ERK activity is being reduced to negligible levels after decreasing the amounts of PDK1.

However, PDK1 seems to exist in an active conformation under normal conditions (Vanhaesebroeck *et al*., 2000). With the hypothesized interaction, one would assume that in the absence of external signals, PDK1 will continuously activate the MAPK pathway, causing uncontrolled growth. This contradicts the current view that the MAPK pathway is activated by external signals. However, simulations show that under serum starved conditions, PDK1 does activate ERK, but its activation is maintained at a low basal level of 0.02% (Figure 10). This suggests that PDK1 may indeed be a necessary but not sufficient condition to fully activate the MAPK pathway, therefore lending support to the presence of the interaction.

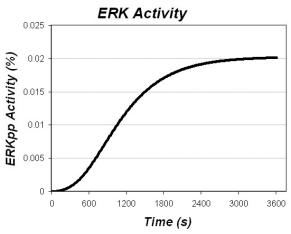

Fig. 10. ERK activation levels in the absence of serum.

We also tested the possibility of *not* having this crosstalk interaction between PDK1 and MEK by removing it from our model. Simulations of this pathway configuration revealed that the ERK activity was kept low throughout even in the presence of serum. This, we suspect, could be due to the inhibitory effect of activated Akt (Moelling *et al*., 2002). To further confirm this observation, we took into account the fact that our model was based on the LNCaP cell line which has defective PTEN due to a frameshift mutation in the *PTEN* gene. Hence we re-simulated the model (with the PDK1-MEK interaction removed) with 10 nM of PTEN. This simulation produced a similar outcome (Figure 11). However, these simulations should not be taken as a conclusive comparison as the modified configuration (without the interaction) could not fit the experimental data.

Although more experiments are needed to confirm the role of PDK1 in the regulation of MAPK activity, the above simulations suggest that the interaction is not only present but also necessary

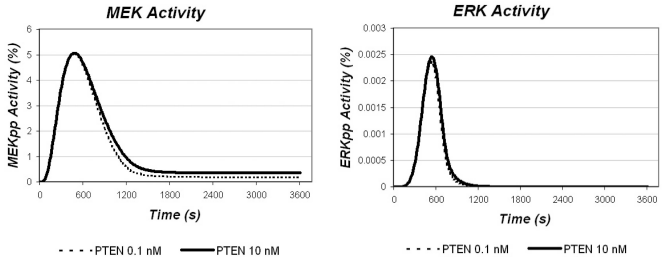

Fig. 11. MEK and ERK activation levels without PDK1 crosstalk.

for enabling the MAPK pathway. This also seems to imply that knocking down PDK1 to reduce Akt activity may affect the proper functioning of the MAPK pathway.

6 DISCUSSION

Decomposition of a large system into smaller sub-systems is an effective way to make the parameter estimation problem manageable. The method proposed here is our first attempt at systematically decomposing dynamical models of signaling pathways. It can be improved in several ways. Currently, we decompose a pathway into components by using the dependency relations among the places and transitions of the HFPN model. For inverse problems such as parameter estimation, information from the downstream components can also possibly aid in constraining the search space for upstream components. At present, we are not taking advantage of this. It should be possible to use techniques such as constraint propagation (Tucker *et al*., 2005) to push up information from downstream components to upstream components.

Also, our decomposition method is most effective when the flow of information is one-way or when the feedback loops are short. If the pathway components are tightly coupled together or if there are long feedback loops, our method may return the entire pathway as the first component. One possible way of dealing with this is to use splines to approximate the concentration profiles of grey places, so that they can be viewed as black places. By doing so, these places can then serve as the boundaries for the smaller components that will be generated.

7 CONCLUSION

In this work, we have built an HFPN model for the Akt and MAPK signaling pathways and investigated their hypothesized crosstalk interaction. Pathway simulation results based on our estimated model parameters exhibit good correlation with experimental data and support a new hypothesized crosstalk mechanism linking the Akt pathway to the MAPK pathway.

One main contribution of this work is a decompositional method for model parameter estimation, based on the HFPN representation. By breaking a large pathway model into smaller, independent components, the new method offers significant improvement in computational efficiency. It shows considerable potential for scaling up to large pathways with hundreds of parameters, a task too daunting for conventional methods. As described in Section 6, there are several improvements that can be made on our current decomposition method, and we are currently working on them. We also plan to extend our approach to other modeling frameworks, such as simultaneous differential equations, hybrid automata, and stochastic Petri nets. The idea is to capture the dependency relations among the pathway elements in the form of a dependency graph similar to the bipartite graph that underlies an HFPN model. On the biological side, it will be important to study the effectiveness of our method on other signaling pathways as well as metabolic and gene regulatory pathways.

ACKNOWLEDGEMENT

We would like to thank Lisa Tucker-Kellogg for fruitful discussions, and the anonymous referees for their valuable comments. D. Hsu is supported in part by NUS grant R252-000-145-112. M.V. Clément is supported by grant R-185-000-106-213 from the National Medical Research Council (NMRC), Singapore.

REFERENCES

Alur,R., Belta,C., Ivančić,F., Kumar,V., Mintz,M., Pappas,G.J., Rubin,H. and Schug,J. (2001) Hybrid Modeling and Simulation of Biomolecular Networks. *Proc. 4th International Workshop on Hybrid Systems: Computation and Control, Lecture Notes in Computer Science*, Vol **2034**, 19-32.

Bellacosa,A., Chan,T.O., Ahmed,N.N., Datta,K., Malstrom,S., Stokoe,D., McCormick,F., Feng,J. and Tsichlis,P. (1998) Akt activation by growth factors is a multiple-step process: the role of the PH domain. *Oncogene*, **17**, 313-325.

Beyer,H.G. and Schwefel,H.P. (2002) Evolution strategies - A comprehensive introduction. *Natural Computing*, **1**, 3-52.

Chaudhary,A., King,W.G., Mattaliano,M.D., Frost,J.A., Diaz,B., Morrison,D.K., Cobb,M.H., Marshall,M.S. and Brugge,J.S. (2000) Phosphatidylinositol 3-kinase regulates Raf1 through Pak phosphorylation of serine 338. *Current Biology*, **10**, 551-554.

Chen,M. and Hofestaedt,R. (2003) Quantitative Petri net model of gene regulated metabolic networks in the cell. *In Silico Biology*, **3**, 347-365.

de Jong,H. (2002) Modeling and Simulation of Genetic Regulatory Systems: A Literature Review. *J. of Comp. Biol.*, **9(1)**, 67-103.

Ghosh,R. and Tomlin,C.J. (2001) Lateral Inhibition through Delta-Notch Signaling: A Piecewise Affine Hybrid Model. *Proc. 4th International Workshop on Hybrid Systems: Computation and Control, Lecture Notes in Computer Science*, **2034**, 232-246.

Hatakeyama,M., Kimura,S., Naka,T., Kawasaki,T., Yumoto,N., Ichikawa,M., Kim,J.H., Saito,K., Saeki,M., Shirouzu,M., Yokoyama,S. Konagaya,A. (2003) A computational model on the modulation of mitogen-activated protein kinase (MAPK) and Akt pathways in heregulin-induced ErbB signaling. *Biochem J.*, **373(2)**, 451-463.

Heldin,C.H. (2001) Signal Transduction: Multiple Pathways, Multiple Options for Therapy. *Stem Cells*, **19(4)**, 295-303.

Henzinger,T.A. (1996) The Theory of Hybrid Automata. *Proc. 11th Annual IEEE Symposium on Logic in Computer Science*, 278-292.

Horoszewicz,J.S., Leong,S.S., Kawinski,E., Karr,J.P., Rosenthal,H., Chu,T.M., Mirand,E.A. and Murphy,G.P. (1983) LNCaP model of human prostatic carcinoma. *Cancer Res.*, **43(4)**, 1809-1818.

Jiang,X. and Cheng,D.C. (2005) A Novel Parameter Decomposition Approach to Faithful Fitting of Quadric Surfaces. *Pattern Recognition: 27th DAGM Symposium, Lecture Notes in Computer Science*, **3663**, 168-175.

Khwaja,A. (1999) Akt is more than just a Bad kinase. *Nature*, **401**, 33-34.

Kimura,S., Hatakeyama,M., Kawasaki,T., Naka,T. and Konagaya,A. (2004) Parameter Estimation for the Simulation of Biochemical Pathways. *Proc. 15th IASTED International Conference on Modeling and Simulation*.

Kikuchi,S., Tominaga,D., Arita,M., Takahashi,K. and Tomita,M. (2003) Dynamic modeling of genetic networks using genetic algorithm and S-system. *Bioinformatics*, **19(5)**, 643-650.

Kirkpatrick,S., Gelatt Jr,C.D. and Vecchi,M.P. (1983) Optimization by Simulated Annealing. *Science*, **220(4598)**, 671-680.

Lincoln,P. and Tiwari,A. (2004) Symbolic Systems Biology: Hybrid Modeling and Analysis of Biological Networks. *Proc. 7th International Workshop on Hybrid Systems: Computation and Control, Lecture Notes in Computer Science*, **2993**, 660-672.

Matsuno,H., Tanaka,Y., Aoshima,H., Doi,A., Matsui,M. and Miyano,S. (2003) Biopathways representation and simulation on hybrid functional Petri net. *In Silico Biology*, **3**, 389-404.

Moelling,K., Schad,K., Bosse,M., Zimmermann,S. and Schweneker,M. (2002) Regulation of Raf-Akt Cross-talk. *The J. of Biol. Chem.*, **277(34)**, 31099-31106.

Moles,C.G., Mendes,P. and Banga,J.R. (2003) Parameter Estimation in Biochemical Pathways: A Comparison of Global Optimization Methods. *Genome Research*, **13(11)**, 2467-2474.

Nicholson,K.M. and Anderson,N.G. (2002) The protein kinase B/Akt signalling pathway in human malignancy. *Cellular Signalling*, **14**, 381-395.

Nagasaki,M., Doi,A., Matsuno,H. and Miyano,S. (2003) Genomic Object Net: I. A platform for modelling and simulating biopathways. *Applied Bioinformatics*, **2(3)**, 181-184.

Neapolitan,R.E. (2003) Learning Bayesian Networks.(1st Ed) *Prentice Hall*.

Pardalos,P.M. and Romeijn,H.E. (2002) Handbook of Global Optimization Volume 2. *Kluwer Academic Publisher*.

Reisig,W. (1992) A Primer in Petri Net Design. *Springer-Verlag*.

Sato,S., Fujita,N. and Tsuruo,T. (2004) Involvement of 3-Phosphoinositide-dependent Protein Kinase-1 in the MEK/MAPK Signal Transduction Pathway. *The J. of Biol. Chem.*, **279(32)**, 33759-33767.

Sorribas,A. and Savageau,M.A. (1988) Strategies for Representing Metabolic Pathways within Biochemical Systems Theory: Reversible Pathways. *Mathematical Biosciences*, **94(2)**, 239-269.

Teong,H.F.C. and Clément,M.V. (2006) Unpublished manuscript.

Tucker,W. and Moulten,V. (2005) Reconstructing Metabolic Networks Using Interval Analysis. *Lecture Notes in Computer Science*, **3692**, 192-203.

Vanhaesebroeck,B. and Alessi,D.R. (2000) The PI3K-PDK1 connection: more than just a road to PKB. *Biochem. J.*, **346**, 561-576.

Voss,K., Heiner,M. and Koch,I. (2003) Steady state analysis of metabolic pathways using Petri nets. *In Silico Biology*, **3**, 367-387.

Williams,B.C. and Millar,W. (1998) Decompositional, Model-based learning and its Analogy to Diagnosis. *AAAI/IAAI*, 197-204.

Ye,P., Entcheva,E., Grosu,R. and Smolka,S.A. (2005) Efficient Modeling of Excitable Cells Using Hybrid Automata. *Computational Methods in Systems Biology*.

Zevedei-Oancea,I. and Schuster,S. (2003) Topological analysis of metabolic networks based on Petri net theory. *In Silico Biology*, **3**, 323-345.